Environmental Pollution 338 (2023) 122674

Contents lists available at ScienceDirect

Environmental Pollution

journal homepage: www.elsevier.com/locate/envpol

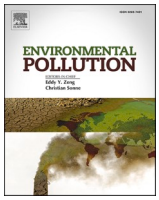

Mixed nitrate and metal contamination influences operational speciation of toxic and essential elements☆

Michael P. Thorgersen [a], Jennifer L. Goff [a], Farris L. Poole II [a], Kathleen F. Walker [b], Andrew D. Putt [b], Lauren M. Lui [e], Terry C. Hazen [b,c,d], Adam P. Arkin [e,f], Michael W.W. Adams [a,*]

[a] Department of Biochemistry and Molecular Biology, University of Georgia, Athens, GA, USA
[b] Earth and Planetary Sciences, University of Tennessee, Knoxville, TN, USA
[c] BioSciences Division, Oak Ridge National Lab, Oak Ridge, TN, USA
[d] Department of Civil and Environmental Engineering, University of Tennessee, Knoxville, TN, USA
[e] Environmental Genomics and Systems Biology Division, Lawrence Berkeley National Laboratory, Berkeley, CA, USA
[f] Department of Bioengineering, University of California at Berkeley, Berkeley, CA, USA

ARTICLE INFO

Keywords:
Sequential extraction
Phosphate
Uranium
Oxyanion
Adsorption
Metal oxides

ABSTRACT

Environmental contamination constrains microbial communities impacting diversity and total metabolic activity. The former S-3 Ponds contamination site at Oak Ridge Reservation (ORR), TN, has elevated concentrations of nitric acid and multiple metals from decades of processing nuclear material. To determine the nature of the metal contamination in the sediment, a three-step sequential chemical extraction (BCR) was performed on sediment segments from a core located upgradient (EB271, non-contaminated) and one downgradient (EB106, contaminated) of the S-3 Ponds. The resulting exchangeable, reducing, and oxidizing fractions were analyzed for 18 different elements. Comparison of the two cores revealed changes in operational speciation for several elements caused by the contamination. Those present from the S-3 Ponds, including Al, U, Co, Cu, Ni, and Cd, were not only elevated in concentration in the EB106 core but were also operationally more available with increased mobility in the acidic environment. Other elements, including Mg, Ca, P, V, As, and Mo, were less operationally available in EB106 having decreased concentrations in the exchangeable fraction. The bioavailability of essential macro nutrients Mg, Ca, and P from the two types of sediment was determined using three metal-tolerant bacteria previously isolated from ORR. Mg and Ca were available from both sediments for all three strains; however, P was not bioavailable from either sediment for any strain. The decreased operational speciation of P in contaminated ORR sediment may increase the dependence of the microbial community on other pools of P or select for microorganisms with increased P scavenging capabilities. Hence, the microbial community at the former S-3 Ponds contamination site may be constrained not only by increased toxic metal concentrations but also by the availability of essential elements, including P.

1. Introduction

Mixed metal contamination of fresh water is often a secondary effect of a larger pollution process that impacts the mobility of elements within the surrounding sediment. In acid mine drainage, exposure of iron-sulfide containing minerals to oxygen, water and iron-oxidizing microorganisms results in acidification and dissolution of the minerals (Simate and Ndlovu, 2014). Depending on the other metal content of these minerals, the impacted groundwater system becomes contaminated with a wide variety of secondary metals (Baker and Banfield, 2003). The use of nitrate-containing fertilizers in agriculture also results in the mobilization of metals that can co-contaminate groundwater used as drinking supply by local populations thereby impacting human health (Ekemen Keskin, 2010; Järup, 2003; Nolan and Weber, 2015). Secondary metal

☆ This paper has been recommended for acceptance by Hefa Cheng.

* Corresponding author. Department of Biochemistry & Molecular Biology, University of Georgia, Athens, GA, 30602, USA.
E-mail addresses: mthorger@uga.edu (M.P. Thorgersen), JLGoff@uga.edu (J.L. Goff), fpoole@uga.edu (F.L. Poole), kfwalker@lbl.gov (K.F. Walker), aputt@lbl.gov (A.D. Putt), lmlui@lbl.gov (L.M. Lui), tchazen@utk.edu (T.C. Hazen), APArkin@lbl.gov (A.P. Arkin), adamsm@uga.edu (M.W.W. Adams).

https://doi.org/10.1016/j.envpol.2023.122674
Received 25 May 2023; Received in revised form 18 August 2023; Accepted 30 September 2023
Available online 2 October 2023

contamination can also impact the composition and function of microbial communities limiting natural bioremediation of contaminated sites (Jiang et al., 2021; Li et al., 2021; Shuaib et al., 2021). Therefore, it is important to understand how contamination sources are impacting the mobility of secondary elements, and what impacts this could have on the surrounding microbial community.

The S-3 Ponds contamination site located within Bear Creek Valley in Oak Ridge, Tennessee, USA is a prime example of such a site where contamination by nitrate and a mixture of metals is impacting the groundwater system. From 1951 to 1983, mixed hazardous waste generated from uranium-processing operations at the Y-12 National Security Complex was disposed in four unlined clay reservoirs, known as the S-3 Ponds, each with a capacity of 9.5 million liters. Acidic uranium nitrate was among the primary wastes deposited at the S-3 Ponds, but waste from remote sites including East Tennessee Technology Park and X-10 sites at ORR, Savannah River site, and Idaho National Engineering Lab was also placed within these reservoirs. In 1983, the waste in the S-3 Ponds was treated by neutralization and sludge was allowed to settle to the bottom before the liquid was removed. The site has since been capped and currently serves as a parking lot (Brooks, 2001). Various groundwater surveys and direct current-resistivity tomography have charted the dispersal of contaminants from the former S-3 Ponds into the surrounding saprolite (Jones, 1998; Revil et al., 2013; Smith et al.). Acidic nitrate contamination extends at least 1500 ft laterally and 45 ft below ground surface (bgs) from the former S-3 Ponds (Jones, 1998) forming 5 distinct plumes (Revil et al., 2013). In addition to the nitrate contamination, several elements are elevated within the contaminated area groundwater, including Fe, Al, Mn, Zn, Ni, Cr, Cu, Co, Pb, As, U, and Cd (Thorgersen et al., 2015). A groundwater survey of 93 wells, including those surrounding the former S-3 Ponds, analyzed 26 geochemical features as well as community structure with 16S rRNA gene sequencing. It was found that microbial communities can serve as quantitative biomarkers for contamination levels, highlighting the impact of the contamination in shaping microbial community composition (Smith et al., 2015).

To study the impact of nitrate and metal contamination on sediment, two sediment boreholes were processed at ORR upgradient (non-contaminated EB271) and downgradient (contaminated EB106) of the former S-3 Ponds (Fig. 1) (Moon et al., 2020). Both cores were analyzed throughout their depth (444 cm bgs for EB271 and 804 cm bgs for EB106) for lithological content, pH, sediment minerology, conductivity, anions, cations, organic acids, biomass, and total elements (Moon et al., 2020). The pH of EB271 varied from 5.62 to 8.01 throughout its depth, while that of EB106 varied from 3.18 to 12.62 with all values for segments deeper than 200 cm bgs being < pH 5.4. Nitrate was typically elevated in EB106 relative to EB271, with maximum concentrations of 2800 mg/L (45 mM) and 83 mg/L (1.3 mM), respectively.

Herein, we expanded upon the previous elemental analysis of the EB271 and EB106 sediment cores using the modified BCR method (Rauret et al., 1999) to sequentially extract selected segments throughout the depth of the two cores. We obtained elemental concentrations for exchangeable (water and acid soluble), reducible and

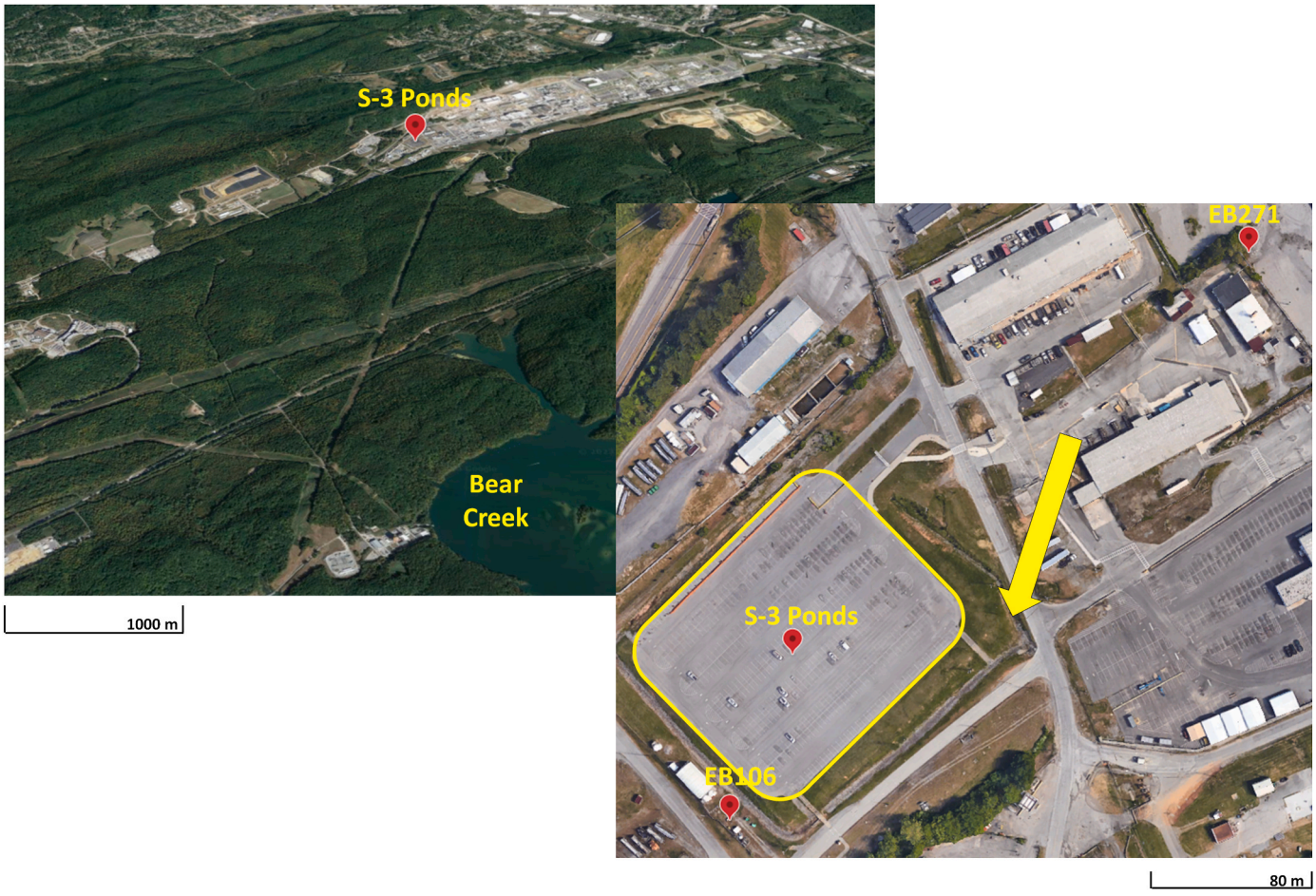

Fig. 1. Location of boreholes EB271 and EB106 in relation to the former S-3 ponds in Bear Creek Valley (Oak Ridge, TN, USA). Locations of boreholes EB271 and EB106 are marked with red pins along with the S-3 ponds that are also highlighted in yellow. The arrow indicates the direction of groundwater flow. Imagery: ©2023 Maxer Technologies/Map data: ©2023 U.S. Geological Survey Google. (For interpretation of the references to colour in this figure legend, the reader is referred to the Web version of this article.)

oxidizable fractions. By comparing the sequential extraction results between the non-contaminated EB271 and contaminated EB106 cores, we observed differential operational speciation for several elements that are likely caused by the low pH, nitrate and mixed metal contamination from the S-3 Ponds. Additionally, we investigated the bioavailability of essential macronutrients, Mg, Ca, and P from the EB271 and EB106 sediment, to three metal-resistant bacteria previously isolated from ORR. Potential impacts of changes caused by the contamination to both toxic and essential element species on the microbial community are discussed.

2. Materials and methods

Sediment Collection. Collection of sediment from cores upgradient (EB271) and downgradient (EB106) of the S-3 Ponds contamination site (Oak Ridge, Tennessee, USA) (Fig. 1) was previously described (Moon et al., 2020). Boreholes were drilled using a dual tube (DT22) direct-push Geoprobe drill rig. The resulting undisturbed sediment encased in polyvinyl chloride liners was segmented into 23 cm segments. After portions of the undisturbed sediment were removed for analyses unrelated to this study (Moon et al., 2020), the remainder of the segments were homogenized and sampled for the extraction experiments described below.

Sequential Extraction of Sediment. Sequential extraction of EB271 and EB106 sediment segments into exchangeable, reducible, and oxidizable fractions was performed using a modified BCR method described previously (Rauret et al., 1999). See supplemental materials and methods for details.

Citrate Bicarbonate Dithionate (CBD) Extraction of Sediment. Extraction of EB271 and EB106 sediment segments by CBD buffer was performed as described previously (Richardson and King, 2018). See supplemental methods for details.

Microwave Digestion. Microwave digestion of sediment samples for total metal analysis was performed as previously described (Ge et al., 2019). See supplemental methods for details.

Sediment Traps. The sediment traps containing non-contaminated ORR sediment were placed in contaminated groundwater well FW106 (35.97729757, −84.2734838). After an 8-week incubation in the groundwater wells, sediment traps were removed, and sediment samples were collected for sequential extraction and microwave digestion as described above.

Element Concentration Determination by ICP-MS. Quantitation of 18 elements by ICP-MS was performed as previously described (Ge et al., 2019). Elements were selected based on known presence in either the native ORR sediment or the S-3 Ponds contamination source.

Strains and Growth Medium. Metal tolerant strains were previously enriched and isolated from the ORR environment in the presence of metal concentrations mimicking the contaminated groundwater surrounding the S-3 Ponds (Thorgersen et al., 2019). *Pantoea* strain sp. MT58 was isolated from non-contaminated sediment (FWB306), while *Serratia* strain sp. MT049 was isolated from a non-contaminated groundwater well (GW066) and *Castellaniella* strain sp. MT123 was isolated from a contaminated groundwater well (FW104).

Base growth medium contained 4.7 mM NH_4Cl, 1.3 mM KCl, 2 mM $MgSO_4$, 0.2 mM NaCl, 1.2 mM $NaHCO_3$, 5 mM NaH_2PO_4, 0.1 mM $CaCl_2$, and 0.2 M MOPS buffer with 1X vitamins and 1X trace elements. For anaerobic growth, 10 mM $NaNO_3$ was added as an electron acceptor. The trace elements were prepared at 1000X concentration and contained 12 mM HCl, 3.8 mM $(NH_4)_2Fe(SO_4)_2{\cdot}6H_2O$, 0.5 mM $ZnCl_2$, 0.5 mM $MnCl_2{\cdot}4H_2O$, 1.5 mM $CoCl_2{\cdot}6H2O$, 0.01 mM $CuCl_2{\cdot}2H_2O$, 0.2 mM $NiCl_2{\cdot}6H_2O$, and 0.2 mM $Na_2MoO_4{\cdot}2H_2O$. The vitamin mix was prepared at 1000X concentration and contained 0.08 mM D-biotin, 0.05 mM folic acid, 0.49 mM pyridoxine HCl, 0.13 mM riboflavin, 0.19 mM thiamine, 0.41 nicotinic acid, 0.23 mM pantothenic acid, 0.74 μM vitamin B_{12}, 0.36 mM p-amino benzoic acid, and 0.24 mM thioctic acid. For growth of *Serratia* sp. strain MT049 and *Pantoea* sp. strain MT58, 20 mM glucose was used as a carbon source, while 20 mM fumarate was used for *Castellaniella* sp. strain MT123. The pH of the medium was adjusted to pH 7.0 using NaOH before filter sterilization for use. For Mg-, P-, and Ca-limited growth medium, base growth medium was prepared with deionized purified water, and $MgSO_4$, NaH_2PO_4, and $CaCl_2$ were not added resulting in concentrations as low as 0.1 μM Mg, 0.6 μM P, and 1 μM Ca. Stock solutions of 1M $MgSO_4$, NaH_2PO_4, and $CaCl_2$ were prepared and diluted to add back Mg, P and Ca as indicated.

Growth Conditions. Growth was monitored in a Bioscreen C (Thermo Labsystems, Milford, MA) by measuring the optical density at 600 nm (OD_{600}). For anaerobic growth, the Bioscreen C was placed in an anaerobic chamber (Plas Labs, Lansing, MI) with an atmospheric composition of 95% Ar and 5% H_2. Growth curves were performed in 400 μL volumes at 25 °C with medium shaking speed in biological triplicate with error bars representing the standard deviation. For growth experiments with sediment samples, the sediment samples for culture amendments were from the saturated zones of EB271 (399 cm bgs) and EB106 (627 cm bgs). The sediment was dried for 24 h at 105 °C before use. Where indicated, 0.2 g of sediment was added to the Mg-, P-, and Ca-limited growth medium cultures (2 mL) in sealed 5 mL vials with a headspace of 20% CO_2 and 80% N_2. Where indicated, Mg, P, and/or Ca were added to the medium in the same concentrations as found in base growth medium. These cultures were grown at 25 °C without shaking for 24 h. Uninoculated control cultures with sediment and concentrations of added Mg, P, and Ca to base growth medium display no growth over the 24 h timespan of the experiment. After growth, 1 mL samples were harvested, and the protein content was determined in μg/mL using the Bradford reagent (Millipore Sigma, Burlington, MA). Experiments were performed in biological triplicate with error bars representing the standard deviation.

3. Results

3.1. Sequential chemical extraction of EB271 and EB106 sediment core segments

Homogenized sediment from selected segments throughout the depth of the EB271 and EB106 cores (upgradient and downgradient of the former S-3 Ponds contamination source) (Fig. 1) was sequentially extracted using the modified BCR method (Rauret et al., 1999). An ICP-MS elemental analysis for 18 different elements was performed on each of the extracted fractions for the core segments. The results are shown in Fig. 2 by depth. Additionally, samples of the sediment segments were extracted with a second CBD reducing method previously used for oxyanion forming elements including P, As, V and Mo (Richardson and King, 2018). A comparison of reducible P, As, V and Mo measured by depth in EB271 and EB106 between the two reducing methods is reported (Fig. S1).

Several elements had concentration peaks at 353 cm bgs in upgradient core EB271 including Mn, Fe, Ca, P, Co, Ni, As, Mo, and Cd (Fig. 2). This depth represents the edge of the capillary fringe and saturated zone. The sequential extraction analyses revealed that this 353 cm bgs peak is predominantly localized to the reducing fraction for Mn, Fe, Co, Ni, As, and Cd. However, similar sized peaks were observed in both the extractable and reducing fractions for Ca and P. In contrast, the Mo peak was primarily localized in the oxidizable fraction. In the total elemental analysis of the EB106 core, a major peak was observed for several elements at 501 cm bgs in the saturated zone (Moon et al., 2020). This saturated zone peak for 14 of the 18 measured elements was primarily localized to the reducing fraction (Fig. 2). In contrast, the 501 bgs peaks for U and Cu were distributed between all three sequentially extracted fractions for EB106, while Al and Cr had peaks at this depth in the reducible and oxidizable, but not, exchangeable fractions.

Comparing EB271 and EB106 sequential extraction fraction profiles, several other observations stand out. The macronutrient elements Mg, Ca, and to a lesser extent P are elevated at most depths in the

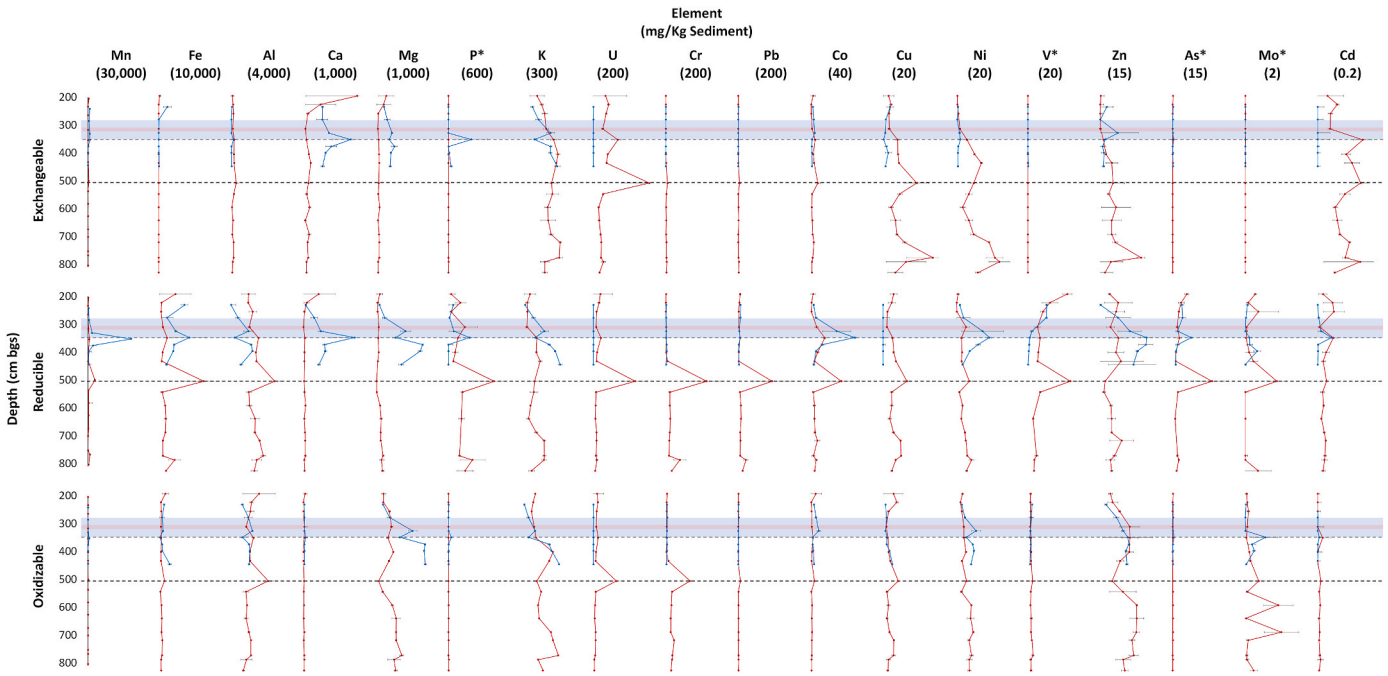

Fig. 2. Sequential extraction of ORR sediment. ORR sediment from boreholes located upgradient (EB271 (blue)) and downgradient (EB106 (red)) of the S-3 Ponds contamination source were subdivided into 23 cm segments before homogenization, sequential extraction and ICP-MS elemental analysis. The upper end of the X-axis range is denoted in parentheses above the graphs for each element. The light blue area indicates the capillary fringe zone for EB271 while the light red area indicates the capillary fringe zone for EB106. The grey dotted line at 353 cm bgs and the black dotted line at 501 cm bgs indicate peak locations for multiple metals in EB271 and EB106, respectively. Error bars show standard deviation for three independently analyzed samples. *The reducible data for these elements was obtained from the citrate bicarbonate dithionite extraction. (For interpretation of the references to colour in this figure legend, the reader is referred to the Web version of this article.)

exchangeable fraction of EB271 relative to EB106. This same trend also holds true for Mg and Ca in the reducible fraction and for Mg in the oxidizable fraction. Several toxic metals known to be present in the contamination plume including Al, U, and Cu were observed at higher concentrations throughout the depth of EB106 compared to what was observed in EB271. Other toxic metals that are associated with the contamination plume, including Pb and Cr, were only elevated in concentration in the EB106 peak at 501 cm bgs.

To further investigate changes in elemental distribution across the sequential extraction fractions (*i.e.,* operational speciation) between the two cores, we compared the sequential chemical extraction data to previously reported total metal extraction data obtained from microwave digestion of the sediment in nitric acid (Moon et al., 2020) (**Table 1**). Four sediment segments were selected, including EB271 353 cm bgs, EB106 501 cm bgs, EB271 444 cm bgs and EB106 627 cm bgs. The former two samples contain the respective reducible fraction concentration peaks of both cores while the latter two samples represent standard saturated zone segments for both cores. Metal oxide forming elements, including Fe, Al, and Mn, were among the most abundant elements by total element analysis in all four sediment segments. Fe is the most abundant in all four segments; however, a large percentage of this Fe (and similarly Al) is not extractable. Less than 1% of the total Fe was detected in the exchangeable fraction of any individual segment. Likewise, in all segments, only around 10% of the total Fe was detected in the reducible and oxidizable fractions together. Mn was more extractable than Fe, with around 10–20% in the exchangeable fractions and high percentages (>40%) in the reducible fraction of all four segments.

Macronutrient elements such as Mg, K, Ca, and P were also among the most highly abundant in the sediment segments by total element analysis. Total Ca was lower in EB106 than EB271 but was highly abundant in the exchangeable fractions (>47%) of all four segments. There was no exchangeable P detected for either EB106 segment. In contrast, 6.6% and 13% of the total P was present in the exchangeable fractions for the EB271 segments. At lower total element concentrations than P in the sediment segments are several elements that are increased in concentration in EB106 due to the contamination plume. These included several micronutrient elements that can be toxic to microorganisms at high concentrations (Co, Cu and V) as well as several non-essential toxic metals (Cr, Pb, As, U and Cd). Of these metals, U had the most dramatic increase in concentration from <2 mg/kg sediment in EB271 segments to 560 mg/kg sediment in EB106 501 cm bgs. The operational speciation of U in EB106 was also changed from that in EB271, with a higher percentage (>35% vs. < 8.6%) in the exchangeable fraction. Increased exchangeability in the EB106 segments is seen for several elements to varying degrees, including K, Ca, Ni, Cr, Cu, Co and Pb. In contrast, several oxyanion forming elements including P, V and As are either undetectable in the exchangeable fraction of EB106 segments or at lower percentages than in the EB271 segments. In a few cases, the percentage of extracted elements was greater than 100%. This could be caused by variation in the homogenized sediment that was sampled and/or indicates that the chemistry of the extraction step released more of the element from the sediment than the total metal determination that used nitric acid.

3.2. Sediment trap and groundwater metal measurements

Both exposure to the contamination plume and sediment lithology (Moon et al., 2020) may contribute to the differences in elemental operational speciation between the two cores. Therefore, we analyzed the operational speciation of non-contaminated ORR sediment both before and after incubation in a highly contaminated groundwater well (FW106 within 2 m of EB106) for 8 weeks (while encased in a sediment trap) (Fig. 3). Several elements known to be present in the former S-3 Ponds contamination source, including Al, K, Zn, Ni, Cr, U and Cd, were elevated in one or more extraction fraction after incubation with the contaminated groundwater. However, as was observed in the sequential extraction data from the two sediment cores, several elements were

Table 1
Comparison of total and sequentially extracted sediment elements for select core segments. Total elements were measured by ICP-MS after microwave digestion in concentrated nitric acid (Moon et al., 2020). The percent exchangeable, reducible, and oxidizable values for each element are in relation to the total microwave digested metals. (Color).

	Total (mg/kg sediment)				% Exchangeable			
	EB271 353 cm bgs	EB271 444 cm bgs	EB106 501 cm bgs	EB106 627 cm bgs	EB271 353 cm bgs	EB271 444 cm bgs	EB106 501 cm bgs	EB106 627 cm bgs
Fe	56000	29000	140000	24000	0.0	0.2	0.0	0.026
Al	7300	18000	21000	16000	2.3	0.2	1.7	0.86
Mg	2200	9100	750	4600	11	2.8	6.6	0.77
K	870	3900	800	1800	8.5	5.0	21	8.2
Ca	1800	700	120	120	47	48	75	120
Mn	7300	410	5400	400	17	23	9.1	19
P[a]	3700	210	2300	230	6.6	13	0	0
Zn	36	69	70	87	3.5	1.2	4.9	3.5
Ni	24	48	32	57	7.3	1.8	20	8.4
Cr	13	38	290	63	0.4	0.3	2.1	2.8
Cu	45	21	100	21	0.4	4.2	12	21
Co	27	19	40	14	4.7	6.9	16	11
V[a]	5.4	16	62	16	0.0	0.4	0	0
Pb	8.2	11	150	13	2.8	0.9	3.4	9.5
As[a]	8.0	1.5	30	1.1	2.4	3.1	0.0053	0
U	1.3	0.35	560	34	1.0	8.6	35	62
Mo[a]	0.062	0.24	1.3	0.061	0.0	0.1	0.17	1.9
Cd	0	0	0.18	0.013	NA	NA	85	530
	% Reducible				**% Oxidizable**			
	EB271 353 cm bgs	EB271 444 cm bgs	EB106 501 cm bgs	EB106 627 cm bgs	EB271 353 cm bgs	EB271 444 cm bgs	EB106 501 cm bgs	EB106 627 cm bgs
Fe	9.7	4.7	5.8	5.2	0.5	6.7	0.76	2.4
Al	3.5	3.9	15	10	11	7.1	12	6.5
Mg	16	5.0	1.3	2.0	16	7.8	5.2	6.2
K	8.9	5.4	9.2	2.3	4.8	5.2	11	5.5
Ca	51	39	22	80	2.2	2.2	21	26
Mn	363	44	78	92	10	6.0	4.4	5.2
P[a]	6.1	0	21	61	0.8	1.1	0	0.68
Zn	34	13	1.9	3.4	20	10	4.5	11
Ni	51	5.4	15	3.6	16	12	12	9.5
Cr	8.4	3.6	50	25	20	5.9	30	27
Cu	0.0	0.0	8.5	12	2.9	16	5.4	6.8
Co	143	15	69	24	7.3	16	8.3	7.6
V[a]	15	0.4	30	15	16	5.6	3.2	9.2
Pb	80	28	82	77	12	6.4	5.4	6.0
As[a]	61	50	35	56	3.6	2.6	0.038	0.83
U	34	22	26	21	20	14	14	16
Mo[a]	236	0.9	83	0	1200	15	36	41
Cd	NA	NA	17	100	NA	NA	6.4	36

[a] The % reducible data for these elements was obtained from the citrate bicarbonate dithionite extraction.

decreased in at least one sediment extraction fraction upon exposure to the contaminated groundwater including Mg and Ca. In the case of P and Mo which tend to form oxyanions in solutions of environmental relevance, negative values were observed for the sediment both before and after incubation in the contaminated groundwater. This indicates that the trace amounts of these elements present in the sequential extraction solutions were adsorbed or incorporated into the sediment in a fashion that could not be extracted in the sequential extraction.

Groundwater from wells located within 2 m of non-contaminated EB271 (GW271) and contaminated EB106 (FW106) had been previously measured for pH, nitrate, and elemental content by ICP-MS in an ORR groundwater survey (Smith et al., 2015) (Table S1). This gives a more homogenized view of the elemental content in the area compared to the spatially resolved depth profiles obtained with the sediment cores. Except for P and Mo (both oxyanion forming elements that had negative values in the sediment trap experiment), all measured elements had higher concentrations in the contaminated FW106 groundwater compared to the non-contaminated GW271 groundwater. This includes Mg and Ca, which were at lower concentrations in the exchangeable fraction of the EB106 core compared to that of EB271. This indicates a difference in the operational speciation changes caused by the contamination for Mg and Ca compared to P and Mo.

3.3. Mg, P and Ca bioavailability for ORR metal tolerant strains

While several elements known to be present in the contamination from the S-3 Ponds were increased in concentration in the exchangeable fraction of contaminated EB106 compared to non-contaminated EB271 (Al, U, Co, Cu, Ni, and Cd). Several other elements, including Ca, Mg and P, are lower in concentration in the exchangeable fraction of EB106 compared to EB271. We therefore examined the degree to which microorganisms from ORR were affected by changes in concentrations of these elements, as reflected in the extraction data. Previously, several metal-tolerant ORR microbes were isolated from ORR under conditions that mimicked the toxic metal concentrations attributable to the former S-3 Ponds contamination (Thorgersen et al., 2019). These strains were previously tested for their resistance to toxic metals present in the contamination, including Cu, Cd, Co, Ni, Mn, U, and Cr (Thorgersen et al., 2019). We selected three of the metal-resistant strains and tested their ability to grow at different concentrations of the macronutrients Mg, P and Ca (Fig. 4). There was variation in the extent to which Mg and P limitation impacted growth of the three strains. However, all three strains did show improved growth in the presence of higher concentrations of Mg (>1 μM) and P (>1 μM). In contrast, Ca limitation did not appear to significantly impact growth of two of the three strains, with only minor increases of growth observed by increasing Ca

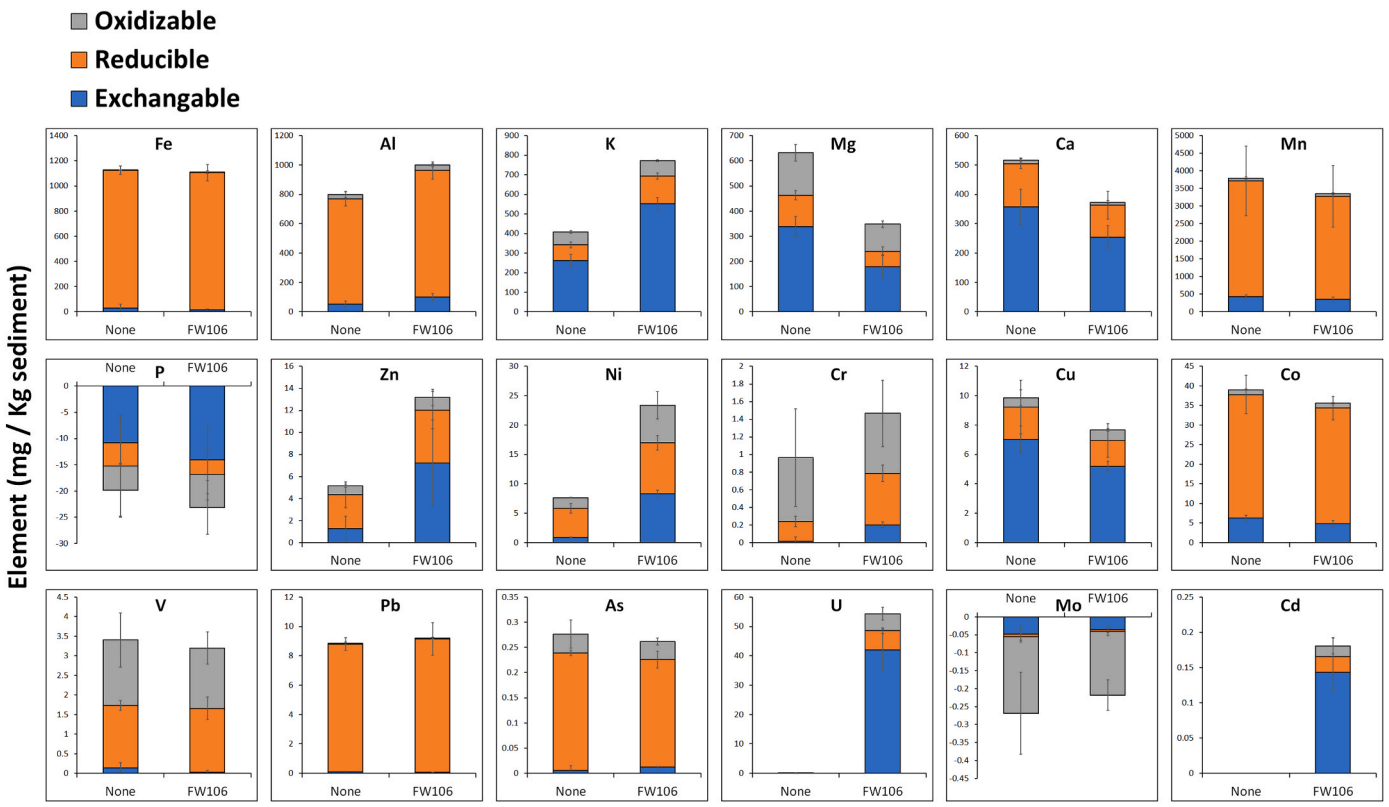

Fig. 3. Impact of contaminated groundwater exposure on operational distribution of sediment elements. Non-contaminated sediment was analyzed using the three-step sequential extraction method before and after an eight-week exposure to contaminated groundwater in well FW106 near borehole EB106 while encased within a sediment-trap. Sediment was extracted to obtain the exchangeable (blue), reducible (orange), and oxidizable (grey) fractions, respectively. Error bars show standard deviation for three independently analyzed samples. The negative values for P and Mo indicate that trace amounts of these elements present in the sequential extraction solutions were adsorbed or incorporated into the sediment in a fashion that could not be extracted in the sequential extraction. (For interpretation of the references to colour in this figure legend, the reader is referred to the Web version of this article.)

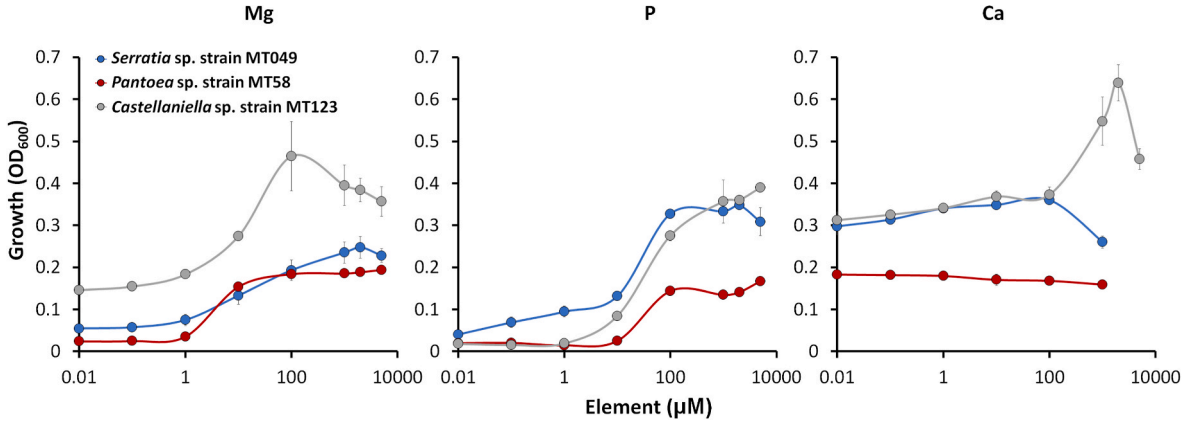

Fig. 4. Growth of ORR metal resistant strains with increasing concentrations of Mg, P, or Ca. ORR metal-resistant strains *Serratia* sp. strain MT049 (blue symbols), *Pantoea* sp. strain MT58 (red symbols) and *Castellaniella* sp. strain MT123 (grey symbols) were grown on media limited for either Mg (left), P (center) or Ca (right, as noted in bold above each graph) with increasing added concentrations of the indicated element. The growth (OD_{600}) reported for each added concentration of Mg, P, or Ca is at the timepoint when the fastest growing condition entered stationary phase for each strain. Error bars show standard deviation for samples in biological triplicate. (For interpretation of the references to colour in this figure legend, the reader is referred to the Web version of this article.)

concentration. Only the growth of *Castellaniella* sp. strain MT123 improved dramatically with the addition of >100 μM Ca (Fig. 4).

We then examined if Mg, P, and Ca from EB271 or EB106 sediment were bioavailable to the metal resistant ORR strains. The three strains were grown on the limiting medium (with indicated additions of Mg, P, and/or Ca) with either (1) no sediment added or (2) sediment added from the saturated zones of non-contaminated EB271 or contaminated EB106 (Fig. 5). At the amounts of sediment added (0.2 g in 2 mL of culture medium), if all the Mg, P, and Ca were bioavailable, the cultures with added EB271 sediment were expected to contain 800 μM Mg, 18 μM P and 388 μM Ca while the cultures with added EB106 sediment were expected to contain 4600 μM Mg, 228 μM P and 17 μM Ca. We found that for all three ORR strains, Mg and Ca from both the EB271 and EB106 sediments were sufficient to support growth, showing that these

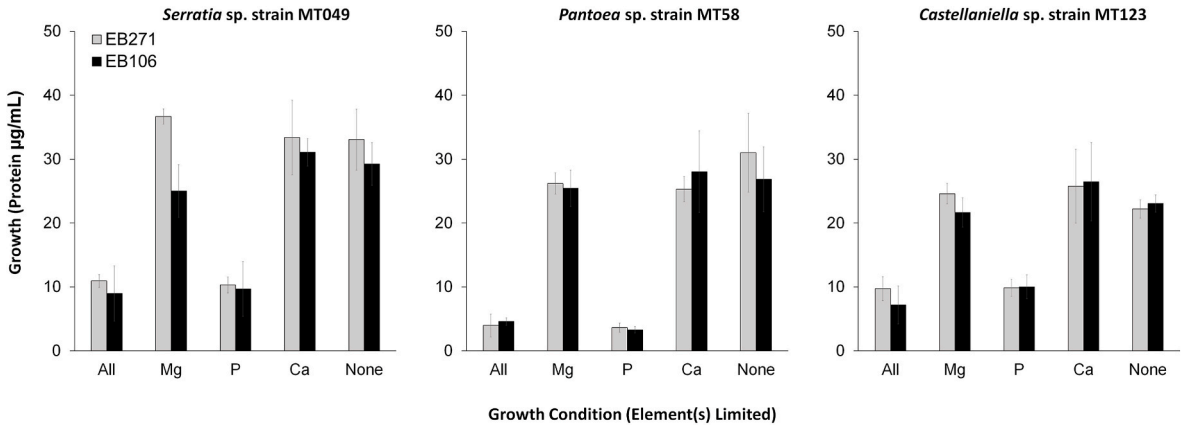

Fig. 5. Bioavailability of Mg, P, and Ca in EB271 and EB106 sediment to ORR metal-resistant strains. ORR metal-resistant strains were grown in media limited for Mg, P and/or Ca with the addition of either sediment from the saturated zone of non-contaminated EB271 or contaminated EB106. After a 24 h incubation, growth was measured using protein content. Error bars show standard deviation for samples in biological triplicate.

two elements are bioavailable from both types of sediment. However, P was not bioavailable for any of the three strains from either sediment sample (Fig. 5), even though what seems to be a sufficient concentration of total P is present in the EB271 and EB106 sediment cultures for growth of the strains (Figs. 4 and 5).

4. Discussion

4.1. Use of sequential extraction techniques

Sequential chemical extraction techniques provide operational speciation information, where the species is defined by the reagent used, that can be useful for evaluating elemental mobility when comparing related environmental samples (Bacon and Davidson, 2008; Brady et al., 2003; Gleyzes et al., 2002). In the modified BCR extraction method, three sequential chemical extractions separate elemental populations based on common naturally occurring complexation states of elements in sediment (Kazi et al., 2005; Rauret et al., 1999). The first acid extraction (exchangeable) dissolves carbonates and contains elements present in the pore water. This fraction is readily available to local microbial communities, as well as plant life. The second is the reducible fraction, which is mainly composed of elements that can be mobilized from metal oxides through chemical or biological reduction. The third or oxidizable extraction releases elements incorporated into stable organic substances (*e.g.,* high molecular weight humics) and is generally not considered to be mobile or bioavailable. Any elements still present in the remaining fraction after the sequential extraction procedure are mainly within crystal lattices of minerals or crystallized oxides and are unlikely to be bioavailable (Basta et al., 2005; Kazi et al., 2005; Bacon and Davidson, 2008; Basta et al., 2005; Gleyzes et al., 2002).

We used the modified BCR method to examine the operational speciation of 18 different elements throughout the depth of sediment cores upgradient (EB271) and downgradient (EB106) of the former S-3 Ponds contamination source at ORR. Elements were selected based on those known to be present in the contamination source (Fe, Al, Mn, Zn, Ni, Cr, Cu, Co, Pb, As, U, and Cd) as well as those commonly present in sediment environments (Mg, Ca, K, and P) or known to be needed for microbial growth (V and Mo). Many of these elements fit into more than one of the stated categories. The modified BCR method (Rauret et al., 1999) was originally used to analyze six metals (Cd, Cr, Cu, Ni, Pb, and Zn). Since then, the method has been used to analyze an increasing array of elements including Al, Mn, Fe, Co, and As (Larner et al., 2006), and even up to 27 elements including K, Mg, Ca, U, P, Mo, and V (Kumkrong et al., 2021). One complication that arises when using the modified BCR method is that oxyanion-forming elements, such P, As, Mo and V can re-adsorb to minerals in the source material that are unaffected by the reducing extraction. This results in erroneously low measurements of these elements for the reducible fraction (Gruebel et al., 1988; Kalyvas et al., 2018). CBD buffer extraction is often used as an alternative reducing method to measure oxyanions adsorbed to metal oxides. This method has been used for the extraction of reducible As (Gruebel et al., 1988), Mo and V (Richardson and King, 2018), and P (Ruttenberg, 1992). A comparison of the BCR and CBD reducible extractions showed that P, As, and Mo in the EB106 core were extracted less efficiently using the BCR reduction step compared to using the CBD extraction. However, the reverse was true for P in the EB271 core (Fig. S1). This highlights the complexity of interpreting operational speciation data and indicates a difference in the interactions between oxyanions and sediment between the two cores.

4.2. Mobility of contaminating metals

As reported previously, the contaminated EB106 core has a peak of multiple metals (Moon et al., 2020) at 501 cm bgs in the saturated zone. With notable exceptions, most of the metals in this peak were extracted primarily in the reducible fraction (Fig. 2). Moon et al. (2020) previously noted increased moisture content and decreased density at this depth in EB106. These physical features likely increased groundwater flow from the contamination source at this depth. There is a second smaller peak of multiple metals at 768 cm bgs in EB106 that could indicate another area of increased groundwater flow. The vertical profiles of the various elements provide insight into the relative horizontal mobility of these elements within the contamination plume. For example, Pb and Cr form sharp peaks at 501 cm bgs while the concentrations of Pb and Cr outside of this segment are like those in non-contaminated EB271 segments (Fig. 2). This indicates that the horizontal mobility of Pb and Cr is less than other elements such as U and Cu, which are elevated in contaminated EB106 compared to EB271 throughout the depth of both cores.

Another observation from the EB106 core is that the highly mobile U was observed at significantly elevated concentrations in all three sequential extractions fractions at all depths (Fig. 2). The aqueous chemistry of U at the S-3 Ponds site includes multiple oxidation states and carbonate complexes affecting solubility in a pH dependent fashion (Brooks, 2001). An excellent example of the solubility changes U can undergo *in situ* in the contaminated ORR subsurface is an investigation where microbial reduction of U stimulated by ethanol and carbonate supplementation was monitored over time (Wu et al., 2006a; Wu et al., 2006b). Soluble U(VI) at the site was reduced to insoluble U(IV) during the supplementation phase of the study. Subsequently, aqueous concentrations of U increased once more when ethanol supplementation was stopped unless carbonate supplementation was also stopped (Wu et al., 2006a; Wu et al., 2006b). High U mobility is observed in many

different types of nitrate contaminated environments. For example nitrate and U co-occur under alkaline and high Ca conditions in the High Plains and Central Valley aquifers (USA) (Nolan and Weber, 2015).

4.3. Mechanisms altering element mobility

The mobility and bioavailability of elements in sediment environments is dependent on the speciation of the elements as well as the surrounding chemical makeup (Bacon and Davidson, 2008; Ure and Davidson, 2008). Metal oxides (*e.g.*, Fe, Al, and Mn oxides) play a large role in controlling the mobility of elements in subsurface environments. The abundance and properties of metal oxides including high points of zero charge, large surface areas, and high density of polar surface functional groups make them ideal for adsorbing both cations and oxyanions (Adegoke et al., 2013; Jenne, 1968; McBride, 1994; Adegoke, 2013). The strength of an adsorptive interaction involving metal oxides can vary greatly depending on the metal oxide and the ion involved ranging from weak electrostatic attraction (outer sphere complexation) to much stronger inner sphere complexation through ligand exchange (Albuquerque et al., 2022; Jain et al., 1999; Peacock and Sherman, 2004; Antelo et al., 2005; Arai and Sparks, 2001; Gimenez et al., 2007).

The sediment at ORR surrounding the former S-3 Ponds is composed primarily of clay minerals coated with Fe, Al and Mn metal oxides (Watson et al., 2004). The EB271 and EB106 cores were previously analyzed by X-ray fluorescence to determine the major oxide component concentrations by depth. Al_2O_3, MnO, and Fe_2O_3 concentrations between the two cores were similar throughout their depths with concentrations varying from about 5 to 25 wt% for Al_2O_3, 0–1% for MnO, and 5–20% for Fe_2O_3 (Moon et al., 2020). The use of the sediment traps herein to control for potential differences in sediment lithology showed commonalities with the sequential extraction results. These included increases in concentrations of extractable sediment associated elements known to come from the S-3 Ponds contamination source (Al, K, Zn, Ni, Cr, U and Cd) and decreased concentrations of extractable sediment associated Mg and Ca.

The macronutrients Mg, Ca, and P and the micronutrient Mo provide interesting points of comparison between the two sites. While there is more exchangeable Mg and Ca in non-contaminated EB271 compared to contaminated EB106 (Fig. 2), both elements are at higher concentrations in the contaminated FW106 groundwater compared to groundwater from non-contaminated GW271 (**Table S1**). These data suggest differential partitioning of Mg and Ca between the solid and liquid phases at the two subsurface sites. In contaminated samples from EB106/FW106, we propose that Mg and Ca are extracted from the sediment by the acidic groundwater, shifting their location from the sediment to the groundwater. P and Mo, on the other hand, appear to be tightly associated with the sediment of both cores. They are the only two elements of the 18 measured that are at lower concentration in the FW106 contaminated groundwater compared to GW271 groundwater (**Table S1**). In addition, both P and Mo were shown to be strongly adsorbed to the ORR sediment in the sediment trap, being pulled from multiple different extraction solutions to associate with the sediment in a fashion that could not be extracted using the BCR method (Fig. 3). Finally, while there was no detectable exchangeable P in the EB106 sediment segments analyzed (**Table 1**), 6.6% and 13% of the total P measured in the two EB271 segments were in the exchangeable fraction (**Table 1**), suggesting distinct speciation patterns of P between the cores. Evidence in support of this was observed comparing reducible P measurements between the BCR and CBD methods. The CBD method greatly improved extraction of P in EB106 sediment, but decreased P detection in EB271 sediment (Fig. S1).

One of the possible reasons for operational differences in elemental populations between the two cores is the impact of pH on the interactions between cations and oxyanions with metal hydroxides. The pH of the groundwater in the contaminated site (a result of the nitrate) is much lower (pH 3.6) compared to the upgradient site groundwater (pH 7.7) (**Table S1**). The adsorption of metal cations such as Pb^{2+}, Zn^{2+}, Cd^{2+}, Cu^{2+} and Co^{2+} has been shown in several cases to decrease with decreasing pH (Feng et al., 2007; Gadde and Laitinen, 1974; Jenne, 1968; Sims and Patrick Jr, 1978). The mobility of these cations in the contaminated environment is potentially aided by the low pH of the contamination. Extractable concentrations for several cations including Al^{3+}, Co^{2+}, Cu^{2+}, Ni^{2+} and Cd^{2+} are elevated at multiple depths in EB106 compared to EB271 indicating that they have traveled to EB106 from the S-3 Ponds (Fig. 2). Unlike the situation for cations, the absorption of elements that form oxyanions under environmental conditions to metal hydroxides including P, As, Cr, Mo, and V typically increases with decreasing pH (Adegoke et al., 2013; Jain et al., 1999; Pérez et al., 2014a, b). This may be one of the factors contributing to the decreased operational availability of P, As and Mo in contaminated EB106 observed throughout the study in the exchangeable fraction (Fig. 2, Table 1). Observation of these elements in the CBD reducible fraction indicate that they are likely adsorbed or incorporated into metal hydroxide minerals from the sediment (Fig. 2, Fig. S1).

Another process occurring at contaminated sites that could affect the operational speciation of several element populations is the precipitation of newly formed metal hydroxides and the resulting co-precipitation of associated ions. Many contaminated sites, like the ORR subsurface, U mill locations and acid mine drainage sites, are both highly acidic near the point source and contaminated with multiple metals (Brooks, 2001; Jönsson et al., 2006; Robertson et al., 2016). As the acidic contamination groundwater at these sites mixes with the surrounding environment and reacts with carbonated soils, it begins to neutralize. As the pH increases, metals in the contamination plume such as Fe, Mg, and Al precipitate out, creating new mineral surfaces for ion adsorption (McBride, 1994; Robertson et al., 2016). This can include the formation of Fe hydroxides minerals like ferrihydrite and goethite (Robertson et al., 2016) that adsorb cations and oxyanions as discussed above. Alternatively, oxyanions can also be incorporated into hydrotalcites, Mg and Al hydroxide minerals that form with increasing pH. Hydrotalcites are composed of metal-hydroxide layers intercalated with the oxyanions (Allada et al., 2002; Ge et al., 2020; Paikaray and Hendry, 2013; Robertson et al., 2016; Smith et al., 2005). These processes can control the mobility and accessibility of oxyanion forming elements including P and Mo and would be expected to decrease their concentrations in the exchangeable fraction shifting them to the reducible or even less operationally available fractions as was observed (Fig. 2, Fig. S1).

4.4. Impact of element mobility shifts on microorganisms

Previously, we investigated how co-precipitation and/or adsorption onto metal hydroxide surfaces decreased the availability of Mo, an essential trace metal for microbial nitrate reduction, in the contaminated ORR subsurface (Ge et al., 2019; Ge et al., 2020). A *Bacillus* strain was isolated from contaminated EB106 sediment that had a high affinity molybdate transporter, potentially aiding survival in the Mo-limiting conditions of the contaminated EB106 sediment (Ge et al., 2020). Herein, we tested the bioavailability of the macronutrients Mg, Ca and P for three metal resistant ORR strains (Fig. 5). While Mg and Ca were bioavailable from both the sediment of either EB271 or contaminated EB106, P was not available from either. Environmental P exists in multiple pools including primary mineral, labile, occluded, soil organic, and plant associated (Vitousek et al., 2010; Walker and Syers, 1976). While we measured changes in labile (exchangeable) and metal oxide bound P in this study (the former of which is decreased in EB106 (**Table 1**) and the latter of which was not bioavailable to the tested strains (Fig. 5)). The decreases in exchangeable P observed for the contaminated EB106 core could increase the dependence of the microbial community at this site on other pools of P such as organic phosphate. Akin to what we found with Mo (molybdate) (Ge et al., 2020), limited availability of P (phosphate) at the ORR site in general could

favor organisms with increased inorganic P scavenging capabilities, such as phosphate-solubilizing bacteria that release organic acids into their local environment to access inorganic phosphate, an advantage that may not exist in the already acidic contaminated environment (Gupta et al., 1994; Olander and Vitousek, 2004; Rodriguez and Fraga, 1999). Future studies focusing on the impact of P limitation to the microbial community in the ORR subsurface are needed to investigate these possibilities.

5. Conclusions

The acidic nitrate and mixed metal contamination from the former S-3 Ponds at ORR has impacted the operational availability and mobility of both toxic and essential elements, the latter of which can also be toxic at high concentrations. While the mobility of some elements from the contamination were limited, certain contamination-associated elements, like U, Cu, and Ni, were found to be highly mobile and to be present in multiple speciation states. However, other essential elements, like P and Mo, were less operationally available at the contaminated site compared to the non-contaminated site. The microbial community at the S-3 Ponds contamination site is impacted by multiple factors including low pH and high toxic metal concentrations (Smith et al., 2015). Limitation of essential oxyanion-forming elements, such as Mo, which is essential for nitrate reduction, and the macronutrient P, which is essential for all microbial life, may also be a constraint on this microbial community impacting the longevity of nitrate in the environment.

Credit author statement

Michael Thorgersen: Conceptualization, Investigation, Writing – Original draft preparation. Jennifer Goff: Methodology, Writing – Review & Editing. Farris Poole: Methodology, Writing – Review & Editing. Kathleen Walker: Methodology Andrew Putt: Methodology Lauren Lui: Methodology, Writing – Review & Editing. Terry Hazen: Supervision. Adam Arkin: Supervision, Funding acquisition. Michael Adams: Conceptualization, Writing – Review & Editing, Supervision.

Declaration of competing interest

The authors declare that they have no known competing financial interests or personal relationships that could have appeared to influence the work reported in this paper.

Data availability

All data are available in the open Mendeley Data Repository

Acknowledgements

This material by ENIGMA (Ecosystems and Networks Integrated with Genes and Molecular Assemblies) (http://enigma.lbl.gov), a Scientific Focus Area Program at Lawrence Berkeley National Laboratory, is based upon work supported by the U.S. Department of Energy, Office of Science, Office of Biological and Environmental Research, under contract number DE-AC02-05CH11231.

Appendix A. Supplementary data

Supplementary data to this article can be found online at https://doi.org/10.1016/j.envpol.2023.122674.

References

Adegoke, H.I., Adekola, F.A., Fatoki, O.S., Ximba, B.J., 2013. Sorptive interaction of oxyanions with iron oxides: a review. Pol. J. Environ. Stud. 22.
Albuquerque, C.G.d., Gavelaki, F., Melo, V.F., Motta, A.C.V., Zarbin, A.J.G., Ferreira, C. M., 2022. Model of inner-sphere adsorption of oxyanions in goethite-Why is phosphate adsorption more significant than that of sulfate? Rev. Bras. Cienc. SOLO 46.
Allada, R.k., Navrotsky, A., Berbeco, H.T., Casey, W.H., 2002. Thermochemistry and aqueous solubilities of hydrotalcite-like solids. Science 296, 721–723.
Antelo, J., Avena, M., Fiol, S., López, R., Arce, F., 2005. Effects of pH and ionic strength on the adsorption of phosphate and arsenate at the goethite–water interface. J. Colloid Interface Sci. 285, 476–486.
Arai, Y., Sparks, D.L., 2001. ATR–FTIR spectroscopic investigation on phosphate adsorption mechanisms at the ferrihydrite–water interface. J. Colloid Interface Sci. 241, 317–326.
Bacon, J.R., Davidson, C.M., 2008. Is there a future for sequential chemical extraction? Analyst 133, 25–46.
Baker, B.J., Banfield, J.F., 2003. Microbial communities in acid mine drainage. FEMS Microbiol. Ecol. 44, 139–152.
Basta, N., Ryan, J., Chaney, R., 2005. Trace element chemistry in residual-treated soil: key concepts and metal bioavailability. J. Environ. Qual. 34, 49–63.
Brady, W.D., Eick, M.J., Grossl, P.R., Brady, P.V., 2003. A site-specific approach for the evaluation of natural attenuation at metals-impacted sites. Soil Sediment Contam. 12, 541–564.
Brooks, S.C., 2001. Waste Characteristics of the Former S-3 Ponds and Outline of Uranium Chemistry Relevant to NABIR Field Research Center Studies. Oak Ridge National Laboratory (US).
Ekemen Keskin, T., 2010. Nitrate and heavy metal pollution resulting from agricultural activity: a case study from Eskipazar (Karabuk, Turkey). Environ. Earth Sci. 61, 703–721.
Feng, X.H., Zhai, L.M., Tan, W.F., Liu, F., He, J.Z., 2007. Adsorption and redox reactions of heavy metals on synthesized Mn oxide minerals. Environ. Pollut. 147, 366–373.
Gadde, R.R., Laitinen, H.A., 1974. Heavy metal adsorption by hydrous iron and manganese oxides. Anal. Chem. 46, 2022–2026.
Ge, X., Thorgersen, M.P., Poole Ii, F.L., Deutschbauer, A., Chandonia, J.-M., Novichkov, P.S., Gushgari-Doyle, S., Lui, L.M., Nielsen, T., Chakraborty, R., 2020. Characterization of a metal-resistant Bacillus strain with a high molybdate affinity ModA from contaminated sediments at the Oak Ridge Reservation. Front. Microbiol. 11, 2543.
Ge, X., Vaccaro, B.J., Thorgersen, M.P., Poole, F.L., Majumder, E.L., Zane, G.M., De León, K.B., Lancaster, W.A., Moon, J.W., Paradis, C.J., 2019. Iron-and aluminium-induced depletion of molybdenum in acidic environments impedes the nitrogen cycle. Environ. Microbiol. 21, 152–163.
Gimenez, J., Martínez, M., de Pablo, J., Rovira, M., Duro, L., 2007. Arsenic sorption onto natural hematite, magnetite, and goethite. J. Hazard Mater. 141, 575–580.
Gleyzes, C., Tellier, S., Astruc, M., 2002. Fractionation studies of trace elements in contaminated soils and sediments: a review of sequential extraction procedures. Trac. Trends Anal. Chem. 21, 451–467.
Gruebel, K.A., Davis, J.A., Leckie, J.O., 1988. The feasibility of using sequential extraction techniques for arsenic and selenium in soils and sediments. Soil Sci. Soc. Am. J. 52, 390–397.
Gupta, R., Singal, R., Shankar, A., Kuhad, R.C., Saxena, R.K., 1994. A modified plate assay for screening phosphate solubilizing microorganisms. J. Gen. Appl. Microbiol. 40, 255–260.
Jain, A., Raven, K.P., Loeppert, R.H., 1999. Arsenite and arsenate adsorption on ferrihydrite: surface charge reduction and net OH-release stoichiometry. Environ. Sci. Technol. 33, 1179–1184.
Järup, L., 2003. Hazards of heavy metal contamination. Br. Med. Bull. 68, 167–182.
Jenne, E.A., 1968. Controls on Mn, Fe, Co, Ni, Cu, and Zn concentrations in soils and water: the significant role of hydrous Mn and Fe oxides. In Trace inorganics in water. Adv. Chem. 73, 337–387.
Jiang, X., Liu, W., Xu, H., Cui, X., Li, J., Chen, J., Zheng, B., 2021. Characterizations of heavy metal contamination, microbial community, and resistance genes in a tailing of the largest copper mine in China. Environ. Pollut. 280, 116947.
Jones, S., 1998. Evaluation of Calendar Year 1997 Groundwater and Surface Water Quality Data for the Upper East Fork Poplar Creek Hydrogeologic Regime at the US Department of Energy Y-12 Plant, Oak Ridge, Tennessee. Oak Ridge Y-12 Plant, Oak Ridge, TN.
Jönsson, J., Jönsson, J., Lövgren, L., 2006. Precipitation of secondary Fe (III) minerals from acid mine drainage. Appl. Geochem. 21, 437–445.
Kalyvas, G., Gasparatos, D., Massas, I., 2018. A critical assessment on arsenic partitioning in mine-affected soils by using two sequential extraction protocols. Arch. Acker. PFL. Boden. 64, 1549–1563.
Kazi, T., Jamali, M., Kazi, G., Arain, M., Afridi, H., Siddiqui, A., 2005. Evaluating the mobility of toxic metals in untreated industrial wastewater sludge using a BCR sequential extraction procedure and a leaching test. Anal. Bioanal. Chem. 383, 297–304.
Kumkrong, P., Mercier, P.H., Gedara, I.P., Mihai, O., Tyo, D.D., Cindy, J., Kingston, D.M., Mester, Z., 2021. Determination of 27 metals in HISS-1, MESS-4 and PACS-3 marine sediment certified reference materials by the BCR sequential extraction. Talanta 221, 121543.
Larner, B.L., Seen, A.J., Townsend, A.T., 2006. Comparative study of optimised BCR sequential extraction scheme and acid leaching of elements in the certified reference material NIST 2711. Anal. Chim. Acta 556, 444–449.
Li, D., Li, G., Zhang, D., 2021. Field-scale studies on the change of soil microbial community structure and functions after stabilization at a chromium-contaminated site. J. Hazard Mater. 415, 125727.
McBride, M.B., 1994. Environmental Chemistry of Soils. Oxford University Press, Oxford.
Moon, J.-W., Paradis, C.J., Joyner, D.C., von Netzer, F., Majumder, E.L., Dixon, E.R., Podar, M., Ge, X., Walian, P.J., Smith, H.J., Wu, X., Zane, G.M., Walker, K.F., Thorgersen, M.P., Poole, F.L., Lui, L.M., Adams, B.G., De Leon, K., Brewer, S.S.,

Williams, D.E., Lowe, K.A., Rodriguez, M.J., Mehlhorn, T.L., Pfiffner, S.M., Chakraborty, R., Arkin, A.P., Wall, J.D., Fields, M.W., Adams, M.W.W., Stahl, D.A., Elias, D.A., Hazen, T.C., 2020. Characterization of subsurface media from locations up-and down-gradient of a uranium-contaminated aquifer. Chemosphere 255, 126951.
Nolan, J., Weber, K.A., 2015. Natural uranium contamination in major US aquifers linked to nitrate. Environ. Sci. Technol. Lett. 2, 215–220.
Olander, L.P., Vitousek, P.M., 2004. Biological and geochemical sinks for phosphorus in soil from a wet tropical forest. Ecosystems 7, 404–419.
Paikaray, S., Hendry, M.J., 2013. In situ incorporation of arsenic, molybdenum, and selenium during precipitation of hydrotalcite-like layered double hydroxides. Appl. Clay Sci. 77, 33–39.
Peacock, C.L., Sherman, D.M., 2004. Vanadium (V) adsorption onto goethite (α-FeOOH) at pH 1.5 to 12: a surface complexation model based on ab initio molecular geometries and EXAFS spectroscopy. Geochem. Cosmochim. Acta 68, 1723–1733.
Pérez, C., Antelo, J., Fiol, S., Arce, F., 2014a. Modeling oxyanion adsorption on ferralic soil, part 1: parameter validation with phosphate ion. Environ. Toxicol. Chem. 33, 2208–2216.
Pérez, C., Antelo, J., Fiol, S., Arce, F., 2014b. Modeling oxyanion adsorption on ferralic soil, part 2: chromate, selenate, molybdate, and arsenate adsorption. Environ. Toxicol. Chem. 33, 2217–2224.
Rauret, G., López-Sánchez, J., Sahuquillo, A., Rubio, R., Davidson, C., Ure, A., Quevauviller, P., 1999. Improvement of the BCR three step sequential extraction procedure prior to the certification of new sediment and soil reference materials. J. Environ. Monit. 1, 57–61.
Revil, A., Skold, M., Karaoulis, M., Schmutz, M., Hubbard, S.S., Mehlhorn, T.L., Watson, D.B., 2013. Hydrogeophysical investigations of the former S-3 ponds contaminant plumes, Oak Ridge integrated field Research challenge site. Tennessee. Geophysics 78, EN29–EN41.
Richardson, J.B., King, E.K., 2018. Regolith weathering and sorption influences molybdenum, vanadium, and chromium export via stream water at four granitoid Critical Zone Observatories. Front. Earth Sci. 6, 193.
Robertson, J., Hendry, M.J., Essilfie-Dughan, J., Chen, J., 2016. Precipitation of aluminum and magnesium secondary minerals from uranium mill raffinate (pH 1.0–10.5) and their controls on aqueous contaminants. Appl. Geochem. 64, 30–42.
Rodriguez, H., Fraga, R., 1999. Phosphate solubilizing bacteria and their role in plant growth promotion. Biotechnol. Adv. 17, 319–339.
Ruttenberg, K.C., 1992. Development of a sequential extraction method for different forms of phosphorus in marine sediments. Limnol. Oceanogr. 37, 1460–1482.
Shuaib, M., Azam, N., Bahadur, S., Romman, M., Yu, Q., Xuexiu, C., 2021. Variation and succession of microbial communities under the conditions of persistent heavy metal and their survival mechanism. Microb. Pathog. 150, 104713.
Simate, G.S., Ndlovu, S., 2014. Acid mine drainage: challenges and opportunities. J. Environ. Chem. Eng. 2, 1785–1803.
Sims, J., Patrick Jr., W.H., 1978. The distribution of micronutrient cations in soil under conditions of varying redox potential and pH. Soil Sci. Soc. Am. J. 42, 258–262.
Smith, H.D., Parkinson, G.M., Hart, R.D., 2005. In situ absorption of molybdate and vanadate during precipitation of hydrotalcite from sodium aluminate solutions. J. Cryst. Growth 275, e1665–e1671.
Smith, M.B., Rocha, A.M., Smillie, C.S., Olesen, S.W., Paradis, C., Wu, L., Campbell, J.H., Fortney, J.L., Mehlhorn, T.L., Lowe, K.A., 2015. Natural bacterial communities serve as quantitative geochemical biosensors. mBio 6.
Thorgersen, M.P., Ge, X., Poole, F.L., Price, M.N., Arkin, A.P., Adams, M.W., 2019. Nitrate-utilizing microorganisms resistant to multiple metals from the heavily contaminated Oak Ridge Reservation. Appl. Environ. Microbiol. 85, e00896-00819.
Thorgersen, M.P., Lancaster, W.A., Vaccaro, B.J., Poole, F.L., Rocha, A.M., Mehlhorn, T., Pettenato, A., Ray, J., Waters, R.J., Melnyk, R.A., Chakraborty, R., Hazen, T.C., Deutschbauer, A.M., Arkin, A.P., Adams, M.W., 2015. Molybdenum availability is key to nitrate removal in contaminated groundwater environments. Appl. Environ. Microbiol. 81, 4976–4983.
Ure, A.M., Davidson, C.M., Eds., 2008. Chemical Speciation in the Environment. John Wiley & Sons, New York.
Vitousek, P.M., Porder, S., Houlton, B.Z., Chadwick, O.A., 2010. Terrestrial phosphorus limitation: mechanisms, implications, and nitrogen–phosphorus interactions. Ecol. Appl. 20, 5–15.
Walker, T., Syers, J.K., 1976. The fate of phosphorus during pedogenesis. Geoderma 15, 1–19.
Watson, D., Kostka, J., Fields, M., Jardine, P., 2004. The Oak Ridge Field Research Center Conceptual Model. NABIR Field Research Center, Oak Ridge, TN.
Wu, W.-M., Carley, J., Fienen, M., Mehlhorn, T., Lowe, K., Nyman, J., Luo, J., Gentile, M. E., Rajan, R., Wagner, D., 2006a. Pilot-scale in situ bioremediation of uranium in a highly contaminated aquifer. 1. Conditioning of a treatment zone. Environ. Sci. Technol. 40, 3978–3985.
Wu, W.-M., Carley, J., Gentry, T., Ginder-Vogel, M.A., Fienen, M., Mehlhorn, T., Yan, H., Caroll, S., Pace, M.N., Nyman, J., 2006b. Pilot-scale in situ bioremedation of uranium in a highly contaminated aquifer. 2. Reduction of U (VI) and geochemical control of U (VI) bioavailability. Environ. Sci. Technol. 40, 3986–3995.